High Sensitivity Refractive Index Sensor Based on Metamaterial Absorber

Wei Zhang*, Jian-Ying Li, and Jian Xie

Abstract—A metamaterial sensor is designed in this paper which can be used to detect the refractive index of an unknown dielectric loaded on the top surface of a metamaterial absorber. The resonant frequency of the absorber will be changed with various refractive indexes of the loaded dielectrics. Especially, the resonant frequency of the sensor is uniquely related to the refractive index of the unknown dielectric with the constant thickness, the linear relation of which is obtained by simulation fitting. A prototype of the absorber is manufactured and measured, which testify the design theory and simulation results. The S_{fre} of the proposed sensor is 0.3537 GHz/RIU, and the FoM can reach 11.0531 RIU^{-1}.

1. INTRODUCTION

Electromagnetic (EM) metamaterial, as a special kind of novel synthetic materials, achieves its dielectric constant and permeability from its structure not normally inheriting them directly from the materials in nature [1]. Smith et al. first achieved the left-hand metamaterial and proved that such a material with special properties is derived from its structure rather than its chemical composition [2]. Due to the strong localization of the EM fields in the vicinity of resonant metallic elements, metamaterials exhibit a strong change of their EM response when a sample material is present [3]. Therefore, metamaterials have important applications in sensors [4]. Refractive index (RI) is an important physical parameter reflecting the intrinsic properties of a material. Therefore, RI sensor has a wide range of applications in petroleum, chemical, biological, food pharmaceutical and environmental monitoring. At present, various ways to detect the refractive index are reported in publications. (1) Surface plasmon polaritons (SPPs) is studied in sensors [5]. Since the surface plasmon resonance (SPR) wavelength is extremely sensitive to the dielectric environment around the metal structure, most SPR-based sensors are usually realized by measuring the wavelength shift of the resonance peak or dip caused by the unit RI, and utilize the figure of merit to characterize the sensing property [6]. However, this detection mode will also bring some further problems. As we know, the SPR wavelength highly depends on the RI of the ambient dielectric, thus a wide RI range of analyte will result in a considerable SPR spectrum shift [7]. It inevitably requires a broad scanning wavelength range of optical detector and may limit the flexible application of the RI sensor. (2) Optical based wireless sensors are developed, but the accuracy is not satisfactory [8]. SiC and Si$_3$N$_4$ based micro-sensors have been introduced in a harsh chemical environment at high temperature, but the complexity of the fabrication process makes it costly [9]. (3) Silicon photonics-based devices have attracted considerable attention because of their high compatibility with on-chip devices. The refractive index sensors in silicon photonics employ directional couplers [10], coupled slot waveguides [11], and micro-ring resonators [12]. These refractive index sensors find wide applications in biosensing and chemical sensing. The optical methods usually used for sensing are the label-based sensing and the label-free sensing. Some of the label-free sensors are refractive index sensor [13] and

gas sensor [14]. Various kinds of waveguide are designed, such as slot, strip and rib waveguides to increase the sensitivity of the sensor [15]. In recent years, slot waveguide structures are widely studied for siliconphotonics based refractive index sensors [16]. However, the fabrication of slot waveguides is difficult, and they exhibit relatively high propagation losses due to side wall roughness [17]. Also, the light coupling is challenging in these nanoscale waveguides [18]. Since the perfect metamaterial absorber has been presented in [19], there is a new approach to design the sensor.

In this paper, the proposed metamaterial absorber consisting of periodical circle rings with two T-type resonators can achieve the absorption over 90% with a high quality factor of 78.90. Because of the strong resonance, the proposed sensor has a high sensitivity of $0.3537\,\mathrm{GHz/RIU}$ with refractive index variation in the range 1.0 to 3.1622, and the FoM is up to $11.0531\mathrm{RIU}^{-1}$. The proposed sensor is a structured composite material possessing sensing properties which are derived from its physical structure but not its constituent material. The structure of the proposed absorber is simple and can be integrated into microwave circuits.

2. ABSORBER DESIGN AND DISCUSS

2.1. Design of the Absorber

A unit cell of the metamaterial absorber is shown in Fig. 1. When the electromagnetic wave is radiated to the surface of the absorber from the free space, a portion of the energy is reflected back into the free space. The wave that enters the inside of the absorber propagates in the form of transmitted wave and then is converted to other forms of energy due to the loss. The absorption of the metamaterial absorber A is:

$$A(f) = 1 - R(f) - T(f) \tag{1}$$

where $R = |S_{11}|^2$, $T = |S_{21}|^2$.

In order to get a perfect absorption, i.e., A is as large as possible, the reflectance and transmittance should be made as small as possible. A metal floor is used to eliminate the transmission as shown in Fig. 1. So the absorption A becomes:

$$A(f) = 1 - R(f) = 1 - |S_{11}|^2 \tag{2}$$

The quality factor Q of the absorber represents the energy storage efficiency of the oscillating system which is defined as [20]:
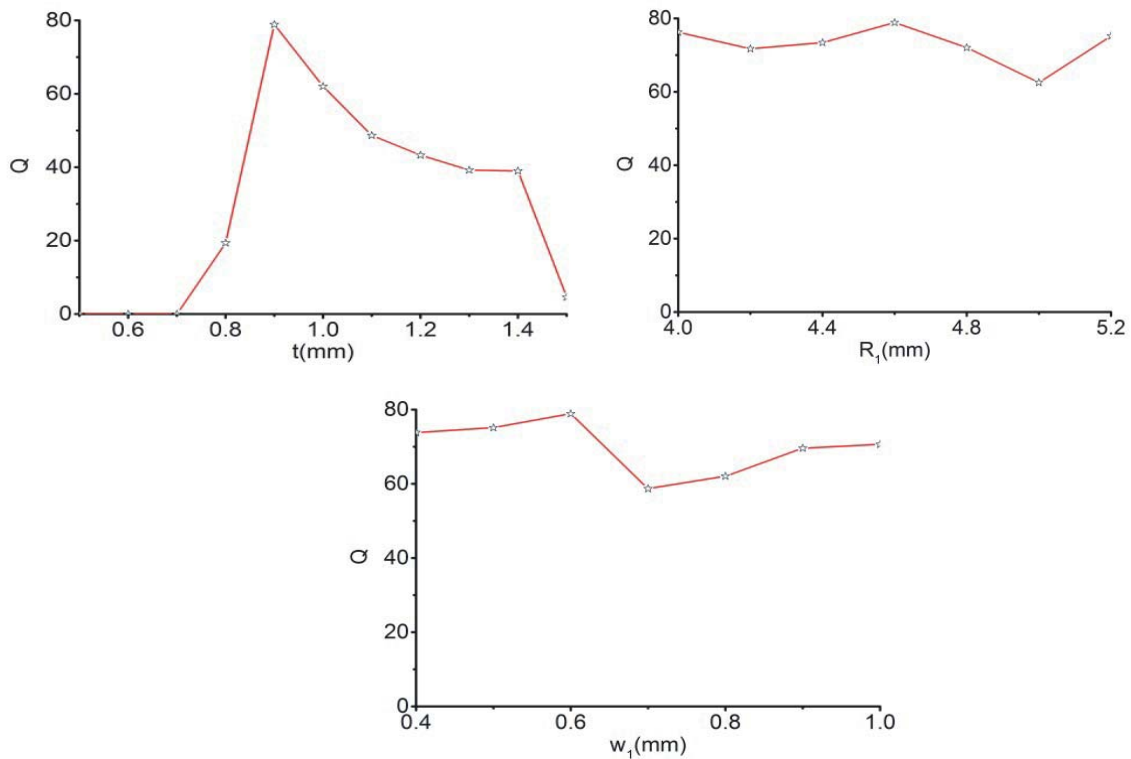
$$Q = f_0/\Delta f \tag{3}$$

where f_0 is the resonant frequency, and Δf is the 3 dB bandwidth.
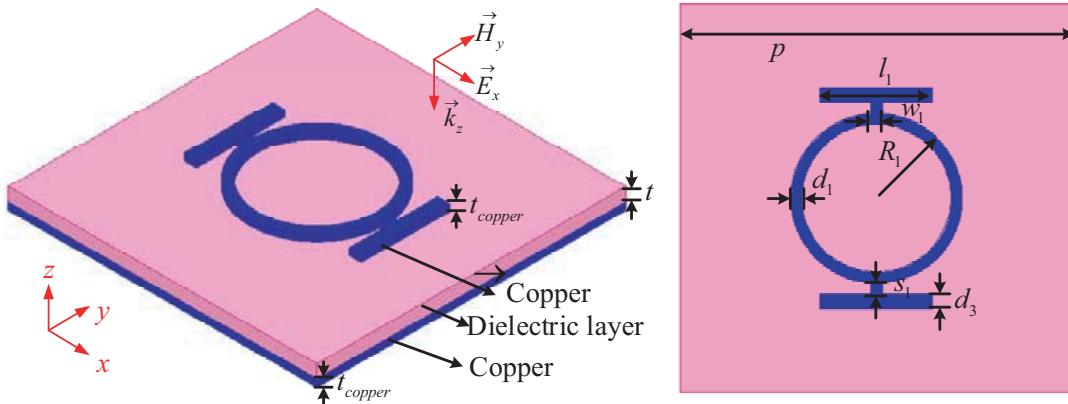
Figure 1. Schematic of a resonance unit cell.

The parameters of the sensor have been optimized in order to get a high Q. The dependences of Q on the thickness of the dielectric layer t, the radius of the ring R_1, and the width of the T-shape w_1 are shown in Fig. 2.

Figure 2. Quality factor dependence on the he thickness of the dielectric layer t, the radius of the ring R_1, the width of the T-shape w_1.

Therefore, the preferable design parameters have been obtained. The metamaterial absorber is designed on a 0.9 mm substrate with the relative permittivity 4.4 and loss tangent 0.02. The top surface of the substrate is the resonance unit cell, and the bottom surface is a metal plate, all of which are coppers with a thickness of 0.02 mm. Dimensions corresponding to the optimized geometry of the resonance unit cell are: $p = 24$ mm, $R_1 = 4.6$ mm, $l_1 = 6$ mm, $d_1 = 0.6$ mm, $d_3 = 0.8$ mm, $w_1 = 0.6$ mm, $s_1 = 0.6$ mm. Considering the normal incidence of the electromagnetic wave in TE mode (polarization angle is 0), the simulation is carried out by ANSYS HFSS. The simulated reflection, transmission and absorption of the absorber are shown in Fig. 3.
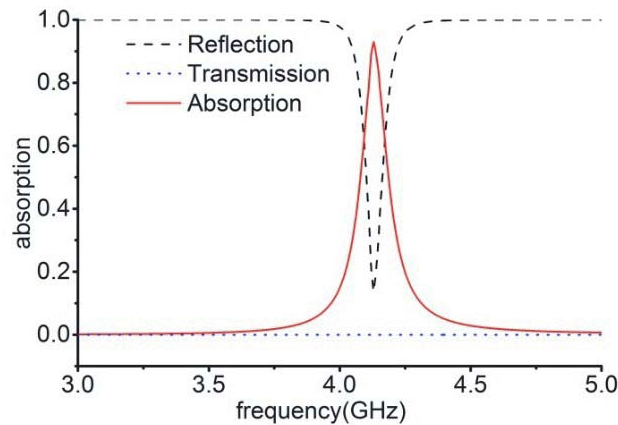

Figure 3. The simulated reflection, transmission and absorption for the absorber while the normally incident light is TE polarized with the electric component along x axis.

The simulation results show that the reflectivity of TE mode wave at resonance frequency is -17.3037 dB, which means that the energy is almost absorbed. As shown in Fig. 3, Q of the absorber is 78.90. The absorption at the resonance frequency 4.13 GHz is over 90%, which can be used as an absorption sensor.

2.2. Absorbing Mechanism

In order to explain the absorbing mechanism, the surface current and power loss density distribution of the absorber at the resonance frequency are further analyzed, as shown in Fig. 4. First of all, as observed in Fig. 4(a), the current is mainly distributed in the metal ring, and the directions is axial symmetric. An equal amplitude reverse magnetic field is generated, so the actual magnetic field represented at the resonance frequency is zero. It is an electric coupling mode. Then, the currents of the upper resonance structure and the lower metal plate are reversed, that is, there is a magnetic response between them. Under the application of an external electric field, the surface current flows along the direction of the arrow, resulting in strong electric resonance. So the energy loss caused by dielectric is enhanced. As shown in Fig. 4(b), the energy loss is the strongest in the T-type section. The reason is that the induced current forms a strong electromagnetic resonance in the metal ring. Finally, a localized electric field between the equivalent capacitances formed by the T-type section is generated, which enhances the dielectric loss.
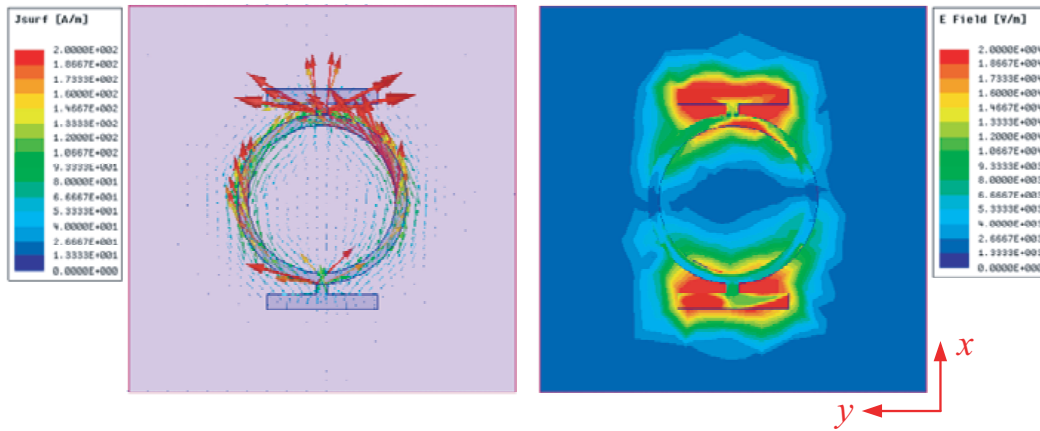
**Figure 4.** The current distributions and electric field distributions at resonance.

3. REFRACTIVE INDEX SENSOR BASED ON THE ABSORBER

3.1. Design of the Sensor

It is necessary to attach the unknown dielectric to the absorber when the refractive index is measured. As shown in Fig. 5, the sensor is able to work because the amplitude and resonant frequency of the absorption curve will change due to the unknown dielectric.

In order to improve the accuracy and sensitivity of the sensor, the appropriate thickness of the unknown dielectric d_0 should be selected. The smaller the influence of d_0 is on the sensor, the better performance the sensor has. The fitting curve between the resonance frequencies of sensors f_0 and d_0 is shown in Fig. 6, under the condition that the relative dielectric constant of the unknown dielectric is 10.

If the unknown dielectric is too thin, the resonance frequency is greatly affected by the thickness, which leads to mistakes and poor reliability. When $d_0 \geq 1.0$ mm the effect becomes gentle, but the over-thickness may reduce the absorption. Considering the sensitivity and size of the sensor, d_0 is set to 1.0 mm.
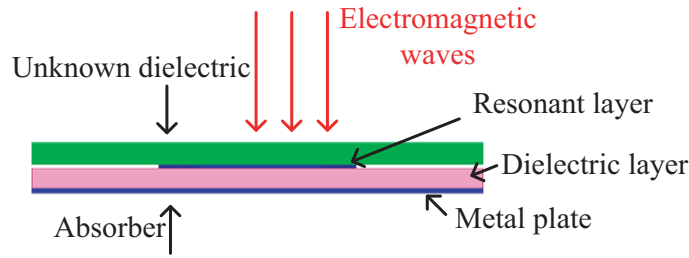
Figure 5. The schematic of the proposed sensor configuration: relative position between absorber and unknown dielectric.
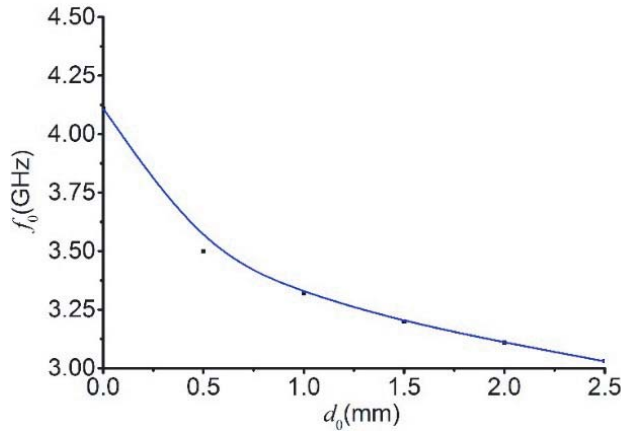
Figure 6. Fitting curve between f_0 and d_0.

3.2. Evaluation of Refraction Index

When d_0 is constant, the absorption of the sensor is uniquely determined by ε_r of the unknown dielectric. The refractive index n can be obtained on account of the relationship between n and ε_r [21]:

$$n = \sqrt{\varepsilon_r \mu_r} \tag{4}$$

In general, the relative permeability μ_r is 1. Therefore, it is expressed as:

$$n = \sqrt{\varepsilon_r} \tag{5}$$

The simulation results of the absorptions are shown in Fig. 7 based on HFSS, where ε_r of the unknown dielectric ranges from 1 to 10.

In order to obtain the functional relation between the refractive index of any unknown dielectric and the resonant frequency of the sensor, the simulation results are linearly fitted by Matlab. The confidence interval is $[1, \sqrt{10}]$ with 95% confidence bound.

The fitting curve is shown in Fig. 8, which can be expressed as:

$$f_0 = -0.3537n + 4.358, \quad 1 \le n \le \sqrt{10} \tag{6}$$

The resonant frequency f_0 drops from 4.130 GHz to 3.322 GHz as the refractive index of unknown dielectric changes from 1 to $\sqrt{10}$. The variance is 0.00301, and the coefficient of determination is 0.9946. It means that the linearity between f_0 and n is very good. The relation between n and f_0 should be refitted instead of seeking its inverse function for error reduction. The confidence interval is [3.322, 4.130] with 95% confidence bound.

$$n = -2.812 f_0 + 12.27 \tag{7}$$

The refractive index of unknown dielectric can be calculated according Eq. (7).
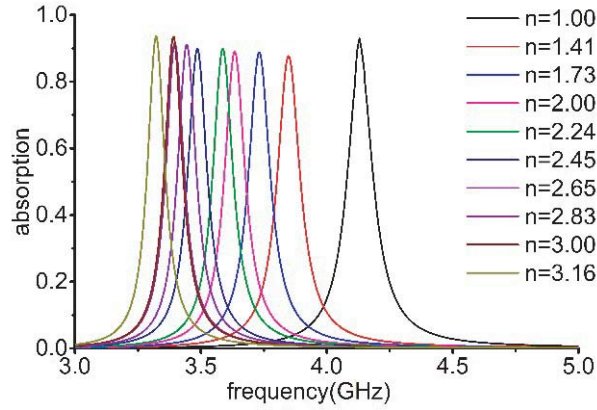
Figure 7. Simulated absorption of the sensor with refractive index from 1.00 to 3.16.
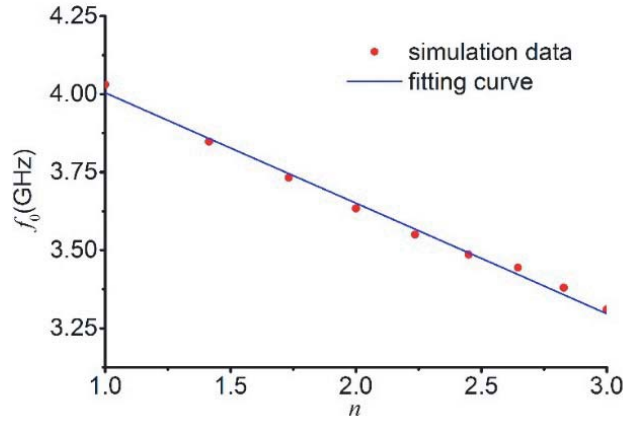
Figure 8. Fitting curve between f_0 and n.

The frequency sensitivity of sensor S_{fre} represents the sensor's ability to detect the change of refractive index [20], which is defined as:

$$S_{fre} = \left| \frac{\partial f_0}{\partial n} \right| \tag{8}$$

It is obtained from Eq. (7) that S_{fre} of the proposed sensor is 0.3537 GHz/RIU (Refractive Index Unit), which is very high. On the other hand, the 3 dB bandwidth Δf can reflect the quality of a resonant peak. The smaller it is, the easier it is to identify the resonant frequency. Therefore, the figure of merit (FoM) is defined as [22]:

$$FoM = \frac{S_{fre}}{\Delta f} \tag{9}$$

The FoM of the proposed sensor can reach 11.0531 RIU^{-1}, while the minimum is 8.8425 RIU^{-1}. The results are quite high, which indicate that the comprehensive performance of the proposed sensor is very good.

4. MANUFACTURING AND TESTING

The dimension of the sensor sample is 360 mm × 360 mm, which contains 16 × 16 unit cells. The sample is shown in Fig. 9(a). PTFE dielectric FR4 ($\varepsilon_r = 4.4$, $\tan \delta = 0.02$) is used to process the absorber. Then the dielectric with known refractive index is used for combined measurement ($\varepsilon_r = 2.55$, $n = 1.5969$,
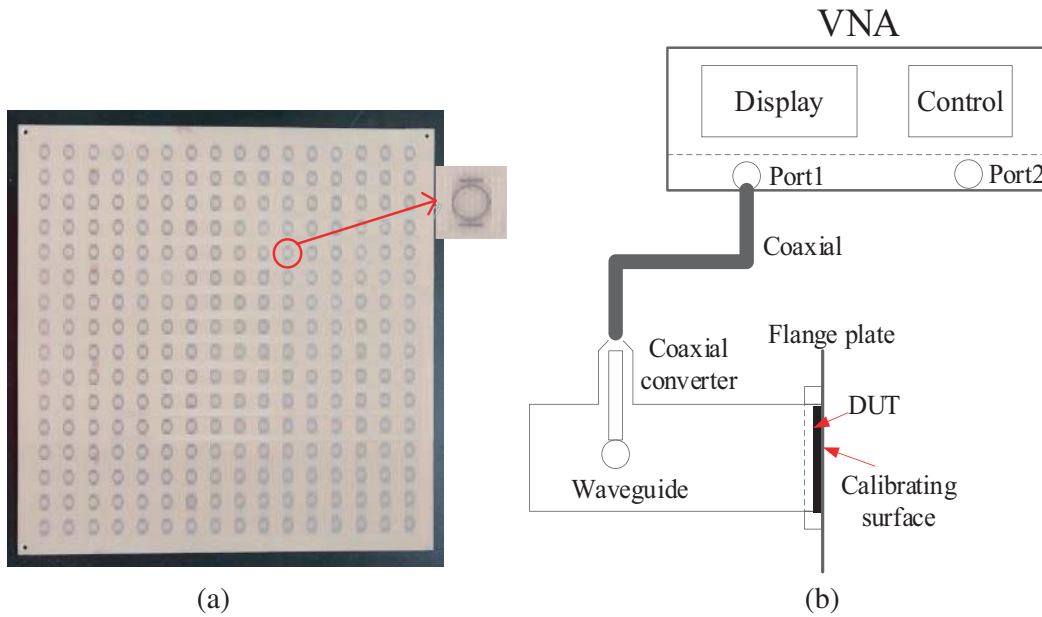
Figure 9. The measurement: (a) The sensor sample with 16×16 unit cells. (b) The measurement method.
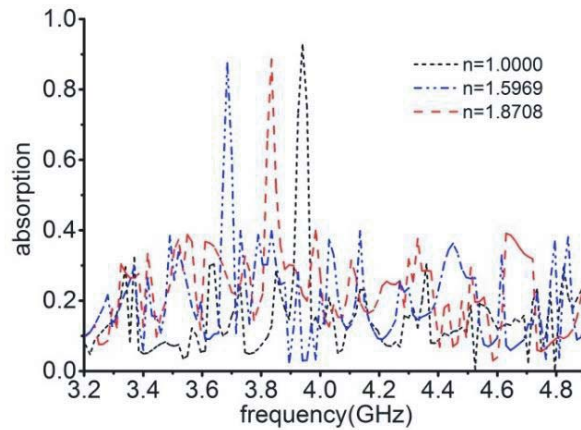
Figure 10. The measured absorption with different dielectric.

and $\varepsilon_r = 3.50$, $n = 1.8708$). The measurement method is shown in Fig. 9(b). A vector network analyzer (VNA) is used to obtain the S parameters. The VNA is connected to the waveguide through the coaxial line. The waveguide is BJ40 (WR-229) to generate the TE_{10} mode wave over the frequency band from 3.22 GHz to 4.9 GHz, which covers the working frequency of the proposed absorber. The TE_{10} mode waves from the waveguide radiate on the sensor and the S parameters can be obtained by the VNA. The de-embedding process is used to eliminate the parasitic effects by equivalent circuit method. S_{11} has been measured, and the absorption can be received and shown in Fig. 10.

When the sensor is used for experiment, the refractive index calculated according to the measured results is compared with the actual refractive index, as shown in Table 1.

It can be seen from the comparison that the refractive index obtained by the fitting relationship of the sensor is in good agreement with the actual refractive index. The absolute error is very small. The main reasons for errors are: (1) Error of fitting curve; (2) The actual ε_r of FR4 used in the sample sensor varies slightly with frequency; (3) There is no seamless connection between the absorber and

Table 1. Actual and measured refractive index of unknown dielectric.

Measured f_0/GHz	Actual n	Measured n
3.974	1.0	1.0947
3.836	1.5969	1.4838
3.688	1.8708	1.8994

the unknown dielectric in the sample sensor; (4) Calculation error and random error in the process and experimentation.

5. CONCLUSION

A refractive index sensor is proposed in the paper, based on a ring resonant absorber. The structure is simple and easy to manufacture, and it is suitable for solid dielectric with RI between 1 and 3.1622. Through data fitting, the complicated physical relationships can be avoided while the accuracy of the estimation can be ensured. S_{fre} of the proposed sensor is 0.3537 GHz/RIU, and the FoM can reach 11.0531 RIU^{-1}. This is a design which combines the absorber and metamaterial sensor phenomena in a simple and efficient manner to provide high-resolution sensing in physical, chemical and biological sensor applications.

REFERENCES

1. Chen, H. T., A. J. Taylor, and N. F. Yu, "A review of metasurfaces: Physics and applications," *Rep. Prog. Phys.*, Vol. 79, 076401, 2016.
2. Smith, D. R., W. J. Padilla, D. C. Vier, S. C. Nemat-Nasser, and S. Schultz, "Composite medium with simultaneously negative permeability and permittivity," *Phys. Rev. Lett.*, Vol. 84, No. 18, 4184–4187, 2000.
3. Cubukcu, E., S. Zhang, Y. S. Park, G. Bartal, and X. Zhang, "Split ring resonator sensors for infrared detection of single molecular monolayers," *Appl. Phys. Lett.*, Vol. 95, No. 4, 189, 2009.
4. Kuhestani, H., M. N. Moghadasi, M. Maleki, and F. B. Zarrabi, "Phase shifter designing base ob hale mode substrate integrated waveguide with reconfigurable quality," *Microw. and Opt. Technology Lett.*, Vol. 57, 2563–2567, 2015.
5. Tan, C., X. Fu, Y. Hu, Y. Deng, X. Shi, S. Zhan, and Z. Xi, "Plasma optical modulation for lasers based on the plasma induced by femtosecond pulses," *Optics Express*, Vol. 25, 14065–14076, 2017.
6. Shen, Y., J. Zhou, T. Liu, Y. Tao, R. Jiang, M. Liu, G. Xiao, J. Zhu, Z. K. Zhou, X. Wang, C. Jin, and C. J. Wang, "Plasmonic gold mushroom arrays with refractive index sensing figures of merit approaching the theoretical limit," *Nature Communications*, Vol. 4, 2381, 2013.
7. Lodewijks, K., R. W. Van, G. Borghs, L. Lagae, and D. P. Van, "Boosting the figure-of-merit of LSPR-based refractive index sensing by phase-sensitive measurements," *Nano Letters*, Vol. 12, 1655–1659, 2012.
8. Lu, X. Y., R. G. Wan, F. Liu, and T. Y. Zhang, "High-sensitivity plasmonic sensor based on perfect absorber with metallic nanoring structures," *Journal of Modern Optics*, Vol. 63, 177–193, 2016.
9. Taniguchi, T., K. Sanbonsugi, Y. Ozaki, and A. Norimoto, "Temperature measurement of high speed rotating turbine blades using a pyrometer," *ASME Turbo Expo 2006: Power for Land, Sea, and Air*, Vol. 2, 521–529, ASME, New York, NY, USA, May 2006.

10. Zappe, S., et al., "High temperature 10 bar pressure sensor based on 3C-SiC/SOI for turbine control applications," *Proc. 1st Nagaoka Int. Workshop Magn. Platform Sci. Technol.*, 753–756, 2000.

11. Dumais, P., C. L. Callender, J. P. Noad, and C. J. Ledderhof, "Silica-on-Silicon optical sensor based on integrated waveguides and micro-channels," *IEEE Photon. Technol. Lett.*, Vol. 17, 441–443, 2005.

12. Nacer, S. and A. Aissat, "Optical sensing by silicon slot-based directional couplers," *Opt. Quantum Electron.*, Vol. 44, 35–43, 2012.

13. Syahir, A., K. Usui, K. Tomizaki, K. Kajikawa, and H. Mihara, "Label and label-free detection techniques for protein microarrays," *Microarrays*, Vol. 4, 228–244, 2015.

14. Fan, X. D., et al., "Sensitivity optical biosensors for unlabeled targets a review," *Anal. Chim. Acta*, Vol. 620, 8–26, 2008.

15. Dikovska, A. Og., et al., "Optical sensing of ammonia using ZnO nanostructure grown on a side-polished optical-fiber," *Sens. Actuators B*, Vol. 146, 331–336, 2010.

16. Topliss, S. M., et al., "Optical fibre long period grating based selective vapour sensing of volatile organic compounds," *Sens. Actuators B*, Vol. 143, 629–634, 2010.

17. Barrios, C. A., "Optical slot-waveguide based biochemical sensors," *Sensors*, Vol. 9, 4751–4765, 2009.

18. Palmer, R., et al., "Low-loss silicon strip-to-slot mode converters," *IEEE Photon. J.*, Vol. 5, 2200409–2200509, 2013.

19. Landy, N. I., S. Sajuyigbe, J. J. Mock, D. R. Smith, and W. J. Padilla, "Perfect metamaterial absorber," *Phys. Rev. Lett.*, Vol. 100, 207402, 2008.

20. Harlow, J. H., *Electric Power Transformer Engineering*, 2–216, CRC Press, 2004, archived from the original on 2016-12-02.

21. Shelby, R. A., D. R. Smith, and S. Schultzr, "Experimental verification of a negative index of refraction," *Science*, Vol. 292, 77–79, 2001.

22. Bencker, J., A. Trüugler, A. Jakab, U. Hohenester, and C. Sönnichsen, "The optimal aspect ratio of gold nanorods for plasmonic bio-sensing," *Plasmonics*, vol. 5, 161–167, 2010.